COVER SHEET

NOTE: This coversheet is intended for you to list your article title and author(s) name only
—this page will not appear on the CD-ROM.

Paper Number:

Title: Statistical Descriptors of Composite Fiber Aggregation

Authors:
Scott E. Stapleton, University of Massachusetts Lowell, Lowell, MA
Jamal F. Husseini, University of Massachusetts Lowell, Lowell, MA
Mathew Schey, University of Massachusetts Lowell, Lowell, MA
Tibor Beke, University of Massachusetts Lowell, Lowell, MA
Evan J. Pineda, NASA Glenn Research Center, Cleveland, OH

(FIRST PAGE OF ARTICLE – align this to the top of page – leave space blank above ABSTRACT)

ABSTRACT

This study introduces a method of characterizing fiber aggregation and resin rich regions in composite microstructures. Microscale models of representative elements (RVE) need to be indicative of the extend of clustering (i.e. close fiber-to-fiber interaction) and resin rich "pools" which may impact the overall strength and performance of a composite structure. This algorithm was used to evaluate different unidirectional 2-D microstructure scans, which will be compared to their manufacturing method or any special treatment processes. These cluster and pool scan statistics can be used as criteria to judge statistical equivalency of artificially constructed microstructures.

INTRODUCTION

Composite structures are susceptible to localized flaws or variability that drives failure initiation. Key geometrical and material characteristics must be taken into consideration when predicting strength and overall response of composites under loading conditions[1–3]. Microstructural characteristics such as fiber orientation, fiber packing, and fiber/matrix material properties can be used to create micro-scale representative volume elements (RVEs) to predict the behavior of the composite. Many current models consider variation of the fiber packing using random fiber generation with fiber neighbors spaced out due to mesh considerations and only consider the global volume fraction when determining statistical equivalency, and find that RVEs converge at very small volumes[4,5]. However, it has been postulated that close/ touching fibers

---

Scott E. Stapleton, Jamal F. Husseini, Mathew Schey & Tibor Beke, University of Massachusetts Lowell, Lowell MA
Evan J. Pineda, NASA Glenn Research Center, Cleveland, OH

and their relation to resin-rich regions may be a driver for failure initiation and propagation, which may require larger volumes for statistical equivalency. Therefore, to make microstructural models that more accurately predict the stress distribution and failure initiation, artificial fiber packings with statistically equivalent fiber distributions considering these vital features may need to be generated.

Many methods have been employed to characterize the fiber packing inhomogeneity of microstructures and the overall global impact it may have on the microstructure[1]. One useful measure is the local fiber volume fraction, which is defined as the fiber volume fraction of the Voronoi cell around a fiber[6]. The distribution of local fiber volume fractions for a microstructure is an important indicator of the inhomogeneity of a microstructure. However, this alone may not be sufficient to describe the microstructure in a way that is meaningful for making transverse strength predictions.

In this work, statistical descriptors of fiber aggregation and dispersion are introduced and their application to several experimental microstructures is demonstrated. The descriptors targeted both densely packed fiber regions ("fiber clusters") and resin-rich ("resin pools") regions, since both can have a large effect on stress distributions and load paths within a microstructure. Using filtering and smoothing, groups of densely packed and sparsely packed fibers were identified, and several metrics describing these groups were identified. Cluster/pool size, orientation, shape, and tightness was extracted from microstructures of several different composites made with different manufacturing methods. A comparison of different manufactured composite microstructure scans are presented using the newly proposed microstructural statistics.

METHOD

In order to identify fiber aggregation ("fiber clusters") and dispersion ("resin pools"), circle detection algorithms of micro-scale images was used to get each fiber's position and radius. A triangulated mesh connecting fibers was generated, and the local fiber volume fraction of each triangle was used determine whether the triangle may be part of a fiber cluster or a resin pool in a filtering process. Then, several rounds of stable subtractive-dominant smoothing was applied to form groups. Finally, the spatial characteristics of these groups was used as a statistical descriptor of the microstructure. The steps are expanded upon in the following sections.

Cluster and Resin Pool Filtering

Delaunay Triangulation creates a nearest neighbor connection between fiber coordinates in a microstructure. This was used rather than the Voronoi cell because of the simplicity of working with triangles. The local fiber volume fraction of the *i*th 2-D triangle is defined as,

$$V_f^i = \frac{A_f}{A_t^i} \tag{1}$$

where A_f is the total area of fibers within the triangle and A_t is the total area of the triangle. A_t is calculated based on its three yz vertex coordinates as,

$$A_t^i = \frac{1}{2}\begin{vmatrix} 1 & y_1 & z_1 \\ 1 & y_2 & z_2 \\ 1 & y_3 & z_3 \end{vmatrix}. \quad (2)$$

The internal angles of a triangle will always be summated to $180°$, therefore the area of fiber within a triangle will consequently be

$$A_f = \frac{\pi}{2} r^2. \quad (3)$$

Assigning each enclosed triangulation, a local volume fraction will yield a distribution over an entire RVE as shown in Figure 1.

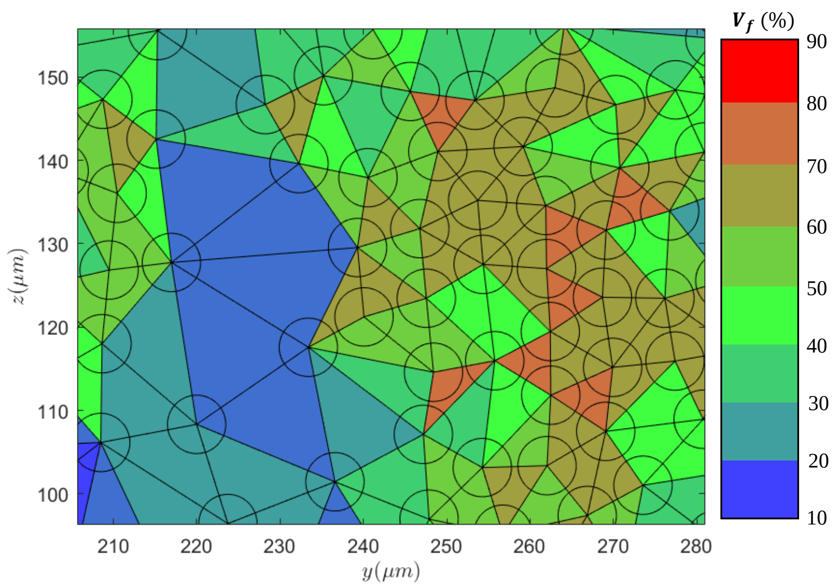

Figure 1. Section of microstructure scan with fibers (black circles) and Delaunay Triangulation (black lines) and assigned volume fractions where blue is more dispersed, green is homogeneous, and red is aggregation.

From Figure 1 it is seen that there are large connected triangles of low volume fraction regions (blue), medium regions (green), and dense packed smaller regions (red). A decision has to be made about which volume fractions belong to which category. For this, Otsu's method of intensity thresholding was utilized[7]. This method essentially creates three bins within the local fiber volume fraction distribution that minimizes the variation within the bins. This method of filtering out volume fractions was utilized in order to avoid assigning static thresholds *a priori*, and divides the space up into three categories.

Identifying Aggregation by Smoothing

While dividing up the microstructural space into three regions is already telling, it does not yet identify whether denser (or more sparse) regions are aggregated together or simply dispersed randomly or homogenously within the microstructure (see Figure 2a). Therefore, a method of smoothing was applied to only keep triangles which belong to group, and to simplify the boundary of such groups. Two filtering methods were used: adaptive and subtractive filtering. The adaptive filtering assigns a triangle be part of a group (or part of the non-group, or background) based on the state of two or more of its direct neighbors. Subtractive filtering only kept a triangle if it was neighboring two or more fibers which were part of a group. The first method removed single triangles and "holes" within groups, while the subtractive filter eliminated small segments that protrude from groups as well as aid in convergence. Multiple rounds of smoothing were required until there are no more possible reassignments to be made, usually 5 or 6 as seen in Figure 2c.

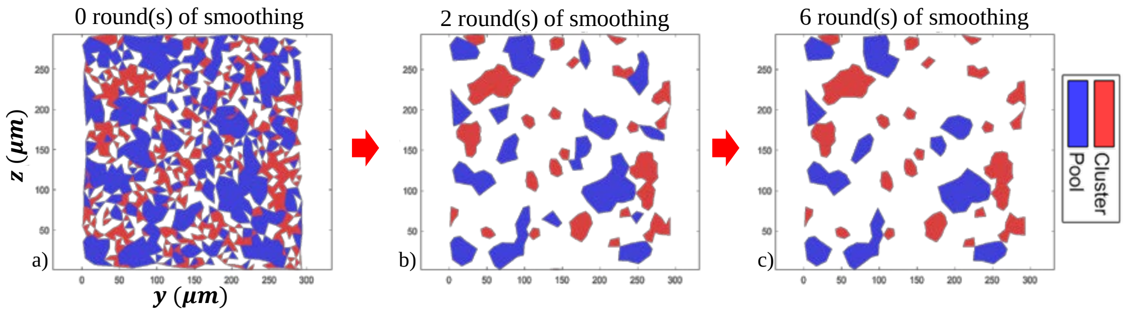

Figure 2. Adaptive and subtractive smoothing for a) no rounds, b) 2 rounds, and c) 6 rounds of smoothing.

Group Descriptors

Once groups of fiber clusters and resin pools are identified, statistical descriptors are used to bring out features of groups within microstructures which may be important. First, the centroid of each triangle is defined as

$$(y_{c_t}, z_{c_t}) = \left(\frac{\sum_{i=1}^{n} y_i}{n}, \frac{\sum_{i=1}^{n} z_i}{n}\right) \tag{4}$$

where (y_{c_t}, z_{c_t}) is the centroid coordinate of each constituent triangle that makes up a cluster or pool, and n is the number of points (for triangles $n = 3$ for the number of vertices). The centroid location of each triangle that composes an entire cluster or pool is averaged and the entire shape centroid is found. The centroid can be used for microstructural reconstruction, but in this study it was not directly compared.

The area moment of inertia or the second moment of inertia describes an object point distribution over a geometrical area. This can tell us whether the group has a particular orientation or whether is more centralized or elongated. The moments of inertia for each group is expressed as I_{yy}, I_{zz}, and I_{yz} and can be arranged in tensor form. The basis can be rotated to find an angle which causes the off-axis terms to vanish ($I_{xy} = 0$). The angle of this rotated coordinate system to the global coordinate system, θ_p, can be found using the equation:

$$\tan(2\theta_p) = \frac{2I_{yz}}{I_{yy} - I_{zz}} \tag{5}$$

and has a bounded range of $-45° \leq \theta \leq 45°$.

The anisotropy of the group was described using R_k. It was defined by

$$R_k = \sqrt{I_{yy}/I_{zz}}. \tag{6}$$

As k approaches 1, the group has more symmetry about the yz axes.

The radius of gyration, R_k, describes how compact vs spread out the group is. It is defined as

$$R_g = \sqrt{\frac{1}{N}\sum_{i=1}^{N}(|\mathbf{x_{ic}}|)^2} \tag{7}$$

where N is the number of triangles in the group and $\mathbf{x_{ic}}$ is the vector connecting the cluster centroid and the *i*th triangle centroid.

Experimental Method

The algorithm was used to process multiple types of microstructures, classified by their manufacturing method, scan type, fiber and matrix type, and any special processes. The inputs for each sample include average fiber radius and positions. Table 1 outlines all sample specifications.

Table 1. Composite Microstructure Sample Specifications.

Sample	Manufacturing	Fiber	Matrix	Special Process	Scan Method
A	VARTM	T700SC	RIMR-135	High Debulk	Serial Sectioning
B	VARTM	T700SC	RIMR-135	Low Debulk	Serial Sectioning
C	VARTM	T700SC	RIMR-135	No Debulk	Serial Sectioning
D	VARTM	TOHO TENAX STS40 F13 48K	RIMR-135	-	Synchrotron
E	Pre-preg/Autoclave	IM7	CYCOM 5320-1	-	Serial Sectioning

RESULTS AND DISCUSSION

Experimental Scan Statistics

The scan along with fiber clustering / resin pool groups are shown in Figure 4. For each experimental scan, the local volume fraction probability density was calculated and is presented in Figure 5. Samples A, B, and C show almost identical distributions while D and E vary greatly. To further characterize each scan, cluster and pool area values are compared in Figure 6.

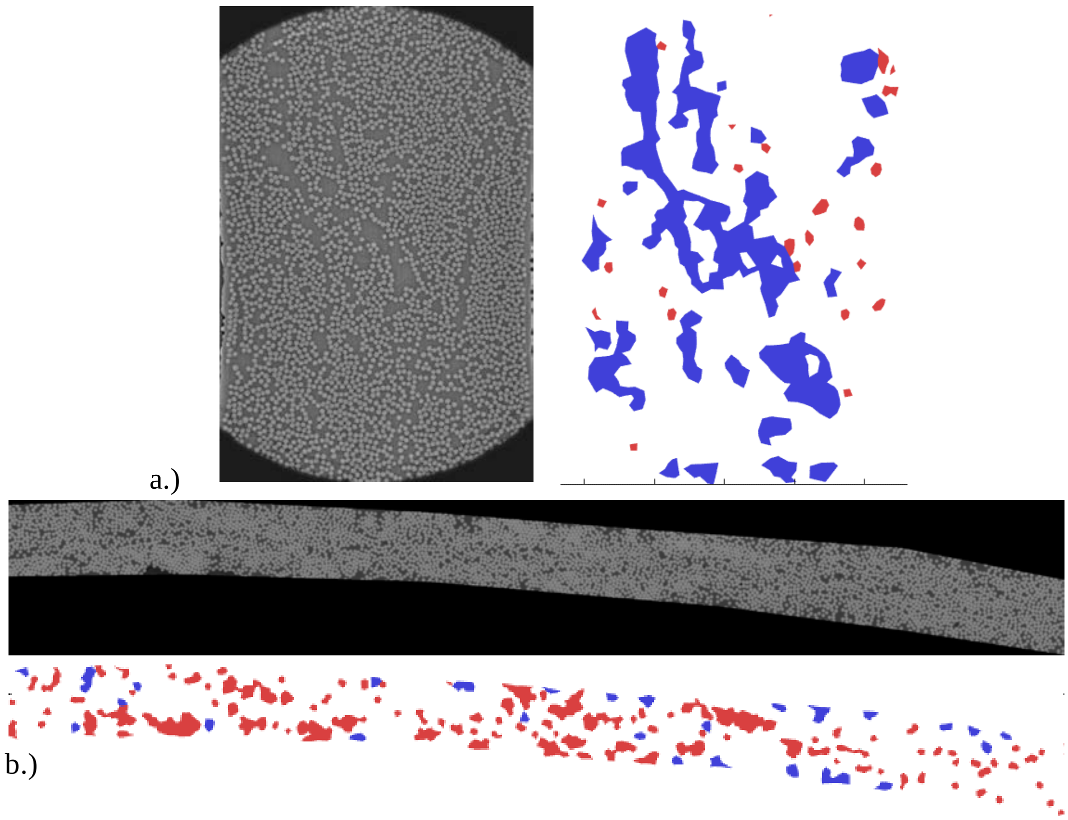

Figure 3. Scans and plot showing fiber clusters (red) and resin pools (blue) for 1) Specimen D and b) Specimen E.

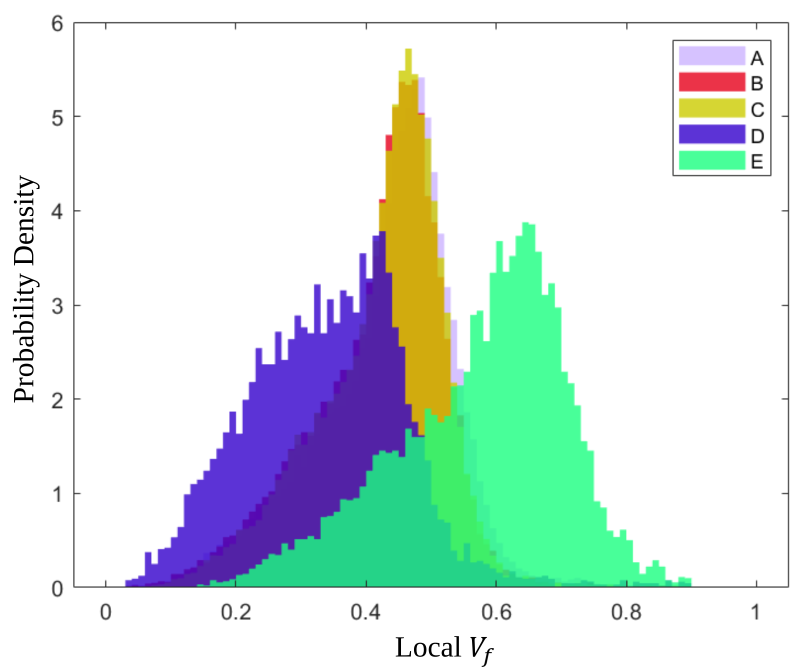

Figure 4. Volume fraction distribution for each experimental scan sample.

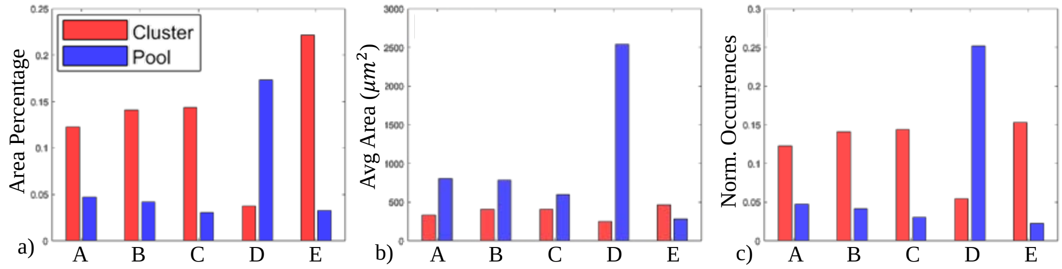

Figure 5. a) Percentage of pool and cluster area, b) average pool and cluster area, and c) number of clusters normalized by the number of fibers and RVE area for each sample.

Figure 4a shows the percentage of cluster and pool area taken up in the entire scan area. Samples A, B, and C show that with less debulking there is a slight increase in clustering and decrease in pooling. Sample D shows a majority of significant resin pooling and E shows significant clustering. The number of groups was normalized by the number of fibers in the scan in Figure 4c. The average cluster and pool area are shown in Figure 4b and are consistent with the reasoning in Figure 4a and 4c. A further representation of the cluster and pool area distribution is seen in Figure 5.

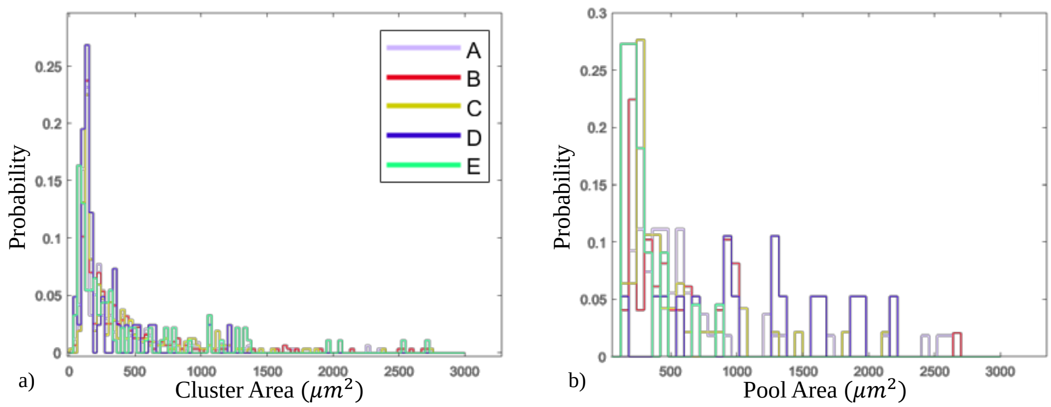

Figure 6. Probability density of a) cluster area and b) pool area distributions.

There are very similar cluster and pool sizes that form across all samples, while the average size may be influenced by large outliers. Descriptors on cluster and pool shape and geometry can be seen in Figure 6.

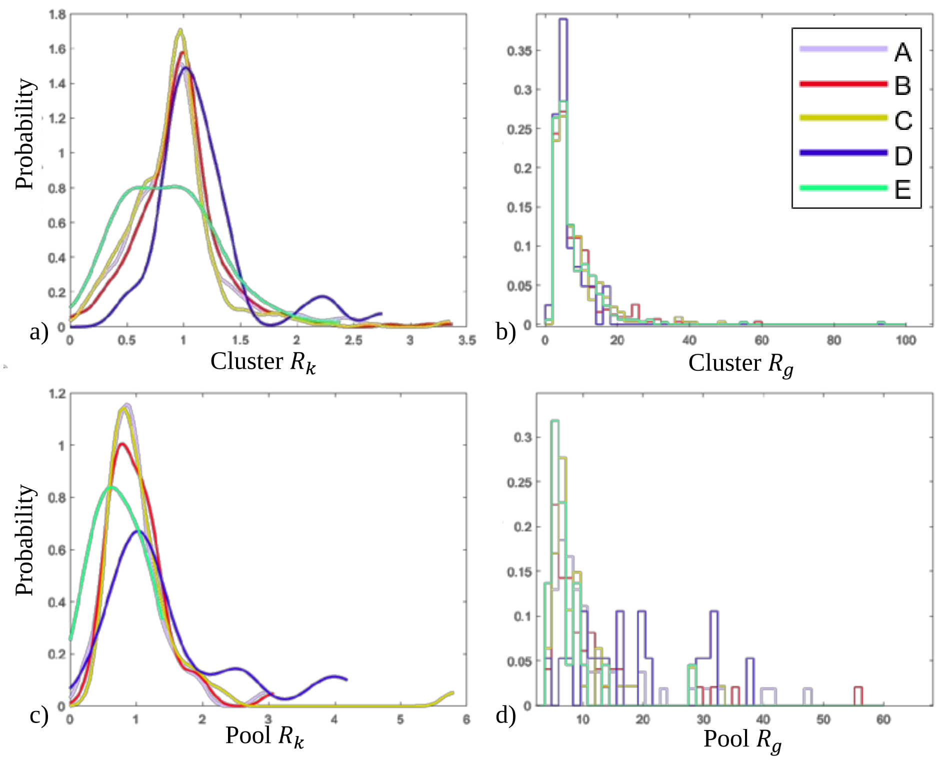

Figure 7. Cluster a) inertia symmetry ratio and b) radius of gyration probability density distribution with pool c) inertia symmetry and d) radius of gyration probability density distribution.

For clusters, Figure 7a describes the distribution of cluster symmetry about its centroid. All samples show a peak around one which is indicative of symmetry, while sample E extends closer to 0.5 which means that some clusters are long along the y axis. Similar trends are seen in Figure 6c for pools. Figures 7b and 7d show the distance from a cluster/ pool centroid to its respective individual constituents. Any trailing edges or outliers indicate a shape that has extending "arms" far away from the centroid.

CONCLUSION

The purpose of this study was to investigate the nature and attempt to quantify the irregularity of fiber distribution in composite microstructures. Sample microstructure scans were sampled for fiber radius and center locations and placed into an algorithm that triangulates and filters fiber triplets based on local volume fractions. This method proved to be promising as well as descriptive in being able to generate statistics about cluster and resin pools shape, size, and orientation. This method is robust enough to capture both extreme clustering and pools within the same microstructure and be comparable to other scans. Now that multiple scans have been run through this process, artificial RVE's can be generated to reproduce similar levels of fiber clusters and resin pools.

REFERENCES

1. Borkowski L, Liu KC, Chattopadhyay A. Micromechanics Model to Link Microstructural Variability to Fiber Reinforced Composite Behavior. In: 55th AIAA/ASME/ASCE/AHS/ASC Structures, Structural Dynamics, and Materials Conference [Internet]. American Institute of Aeronautics and Astronautics; 2014 [cited 2020 Jul 17]. (AIAA SciTech Forum). Available from: https://arc.aiaa.org/doi/10.2514/6.2014-0155

2. González EV, Maimí P, Camanho PP, Lopes CS, Blanco N. Effects of ply clustering in laminated composite plates under low-velocity impact loading. Composites Science and Technology. 2011 Apr 12;71(6):805–17.

3. Mishnaevsky L, Dai G. Hybrid carbon/glass fiber composites: Micromechanical analysis of structure–damage resistance relationships. Computational Materials Science. 2014 Jan 1;81:630–40.

4. Bednarcyk BA, Aboudi J, Arnold SM. Analysis of fiber clustering in composite materials using high-fidelity multiscale micromechanics. International Journal of Solids and Structures. 2015 Sep 1;69–70:311–27.

5. Pathan MV, Tagarielli VL, Patsias S, Baiz-Villafranca PM. A new algorithm to generate representative volume elements of composites with cylindrical or spherical fillers. Composites Part B: Engineering. 2017 Feb 1;110:267–78.

6. Fast T, Scott AE, Bale HA, Cox BN. Topological and Euclidean metrics reveal spatially nonuniform structure in the entanglement of stochastic fiber bundles. J Mater Sci. 2015 Mar 1;50(6):2370–98.

7. Xu X, Xu S, Jin L, Song E. Characteristic analysis of Otsu threshold and its applications. Pattern Recognition Letters. 2011 May 1;32(7):956–61.